



ISSN: 2395-7852



# International Journal of Advanced Research in Arts, Science, Engineering & Management (IJARASEM )

Volume 11, Issue 1, January 2024



INTERNATIONAL  
STANDARD  
SERIAL  
NUMBER  
INDIA

**IMPACT FACTOR: 6.551**

[www.ijarasem.com](http://www.ijarasem.com) | [ijarasem@gmail.com](mailto:ijarasem@gmail.com) | +91-9940572462 |

# Abrasive Failures on High Stress Grinding and Free Particles Influences

**Dr. Baddham Sairam Goud**

Assistant Professor, Brilliant Institute of Engineering & Technology, Hyderabad, Telangana, India

**ABSTRACT:** Wear, a form of surface deterioration, is a factor in a majority of component failures. Adhesive wear, the type of wear that occurs between two mutually soluble materials, is also discussed, as is erosive wear, liquid impingement, and cavitation wear. The article also presents a procedure for failure analysis, jaw-type rock crusher wear, electronic circuit board drill wear, grinding plate wear failure analysis, impact wear of disk cutters, and identification of abrasive wear modes in martensitic steels. Abrasive wear affects the mechanical properties of materials used in high-temperature pneumatic systems. A finite element model for simulating the abrasive wear process and its effects on materials are being developed as part of the research. The abrasive particles' properties, the temperature distribution of the materials, and the mechanics of contact between the abrasive particles and the materials will all be taken into account by the model.

**KEYWORDS:** Abrasive wear, grinding plate, high temperature, abrasive particles, materials

## I. INTRODUCTION

Abrasive wear is the type of wear mechanism that results in the disintegration of the material on the surface due to the influence of the hard particle in contact with the surface. It also occurs when a hard surface or particles interacts or slides on the soft surface and causes material loss. This is a type of the wear that occurs due to the loading of solid particle on the surface of the material which is having hardness that is equal or lesser compared to the loaded particle.

Abrasive wear occurs when a hard rough surface slides across a softer surface; in this case, wear is defined as damage to a solid surface that generally involves progressive loss of material and is due to relative motion between that surface and a contacting substance or substances. Abrasive wear is commonly classified according to the type of contact and the contact environment; the type of contact determines the mode of abrasive wear. The two modes of abrasive wear are known as two-body and three-body abrasive wear. Two-body abrasive wear occurs when one surface (usually harder than the other) cuts material away from the other surface; this mechanism very often changes to three-body abrasion as the wear debris then acts as an abrasive between the two surfaces. Three-body wear occurs when particles are not constrained, but are free to roll and slide down a surface.

The most common mechanisms of abrasive wear are plowing, cutting and fragmentation. Plowing is the mechanism by which, during the formation of grooves, material is not directly removed but is displaced to the side, resulting in ridges adjacent to grooves, which may be removed by subsequent passage of abrasive particles. During cutting, material is taken away from the surface as primary debris, in the same way as machining. Fragmentation is a type of wear typical for brittle materials due to indentation followed by crack propagation.

Abrasive wear is a complex phenomenon and there are many variables to be taken into account, such as the wear environment, the type of motion, and the contact forces. Changing one variable can change the outcome of the tests substantially. An essential variable in abrasive wear is the abrasive itself and its properties. The abrasive is in a big role largely determining the mechanisms with which the wear is happening. The effects of size and shape of the abrasives on wear have been discussed by several authors. The same abrasive properties may have different effects when conditions change, for example, from impacts to abrasion. On the other hand, different wear mechanisms can be observed in systems where the conditions are similar and only the abrasive type is varied

### **Abrasive wear due to micro-cutting**

The first mechanism which represents the classic model of abrasive wear formation is the cutting where the sharp grit or asperity causes the cut on the softer material surface resulting in wear. The worn-out material from the softer material surface is called the wear debris. This mechanism of micro-cutting is shown in the below Figure.

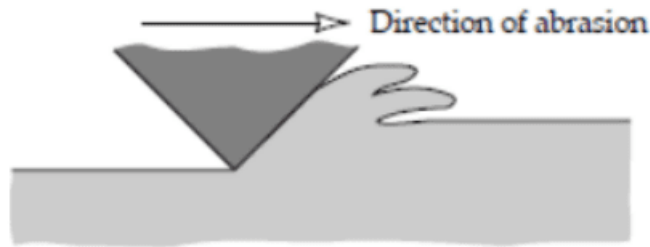


Figure: Abrasive wear by cutting

The two modes of abrasive wear are two-body and three-body abrasive wear. In two-body abrasion, wear is caused by hard protuberances on one surface which can only slide over the other; whereas in three-body abrasion, particles are trapped between two solid surfaces but are free to roll and slide. The schematic diagram illustrating the mechanism of 2- body abrasive wear and 3-body abrasive wear is shown in Figure. The rate of material removal in 3-body abrasion is one order of magnitude lower than that for 2-body abrasion. This is because the loose abrasive particles abrade the solid surfaces for only about 10% of the time during sliding, while they spend about 90% of time in rolling. Most of the abrasive wear problems, which arise in agricultural and industrial equipment, are 3-body, while 2-body abrasion is encountered primarily in material removal operations.

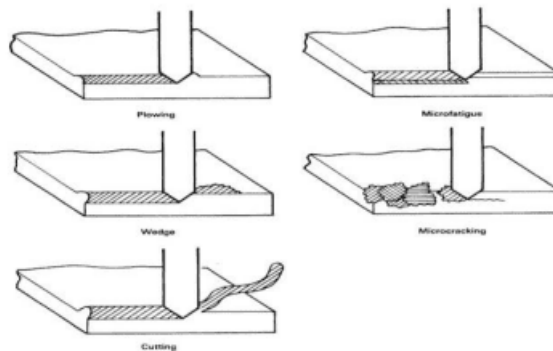


Figure : Mechanism of abrasive wear

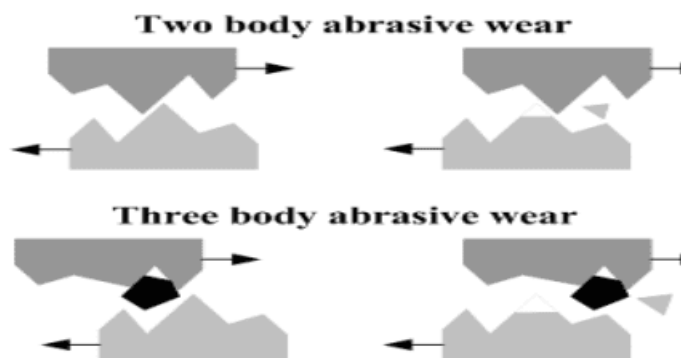


Figure : Two-body and Three-body abrasive wear

A 3-body dry abrasive wear testing machine is based on the principle of rolling and sliding of particles down a moving surface. The testing machine is based on parameters described by ASTM G-65 for dry sand rubber wheel test. Aluminium alloys are designated according to their major alloying elements. The 3xx group contains silicon as the primary alloying element. This is because it increases the fluidity of the melt, reduces the melting temperature, decreases the shrinkage during solidification and is relatively inexpensive



## II. METHODOLOGY

To study the high stress abrasive wear behaviour a two-body abrasive wear testing system was set up in the laboratory. This model is known as the pin-on-drum machine, and it simulates the practical work conditions.

The pin-on-drum machine is constituted as shown in the Figure 4.4. The pin specimen is 6 mm in diameter, with an allowable length of 20mm to 35mm. The pin can be adjustable with a screw on the top of the specimen holder, so that it can make full contact with the drum. The rotating drum is 86mm in diameter with a length of 300mm, and is driven by a variable speed electric motor through two gear boxes I and II.

When the drum rotates, the entire surface of the specimen continuously comes in contact with a virgin abrasive paper along a helical path. The wear path for the test is selected as 6m for which the horizontal distance of specimen movement is 181.8mm.



Figure: Photograph of the pin-on-drum machine

Table: Design data for pin-on-drum machine

Machine Parts	Data
Motor	Variable speed 60-200 rpm
Gear Box-I Motor	Speed reduction ratio $i_1=1:10$
Gear Box-II-Gear-Speed reduction ratio	$Z_1 = 20, Z_2 = 40, Z_3 = 180, Z_4 = 22$ $i_2 = Z_1/Z_3 = 1:9, i_3 = Z_3/Z_4 = 90:11$
Guide screw	$t_s = 1 \text{ mm}$
Drum	$D = 86 \text{ mm}, L_D=300 \text{ mm}$
Pin	$d = 6 \text{ mm}, l=20-35 \text{ mm}$

### SPECIMEN PREPARATION FOR MICROSCOPY

Optical and Scanning electron microscopy was done to examine the microstructures of the monolithic materials and the WC/Co powders and coatings. A small section of the monolithic materials was mounted in bake lite and metallographic specimens were made by hot compression. Cross sections of the WC-Co coatings were prepared using a high speed cutting wheel, and mounted using epomet and bake lite (1:1). The powder cross sections were prepared by first mounting very thin layers of the powders in bake lite, and then light polishing on a 1200 grit paper. The monolithic materials were hand ground using 180, 240, 320, 400, 600, 800 and 1200 grit abrasive papers and then polished on a 6µm and 1µm diamond wheel. For polishing the WC-Co coatings the following procedure was adopted. Grinding and polishing operations were done using an Abramin automatic polishing machine. A 40µm diamond grinding disc was used for 20 minutes. This was followed by polishing on a 6µm diamond polishing pad using a pan-w napless cloth (duration: 27 minutes), followed by polishing on 1µm diamond polishing pad for 5 minutes, and finally using a Metal diDPNap cloth for 1/4µm polishing (duration : 2 minutes). A pressure of 200N was applied, and the rpm was maintained at 300, during all the operations.



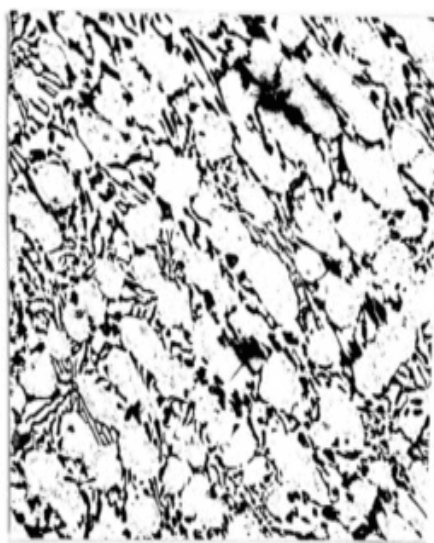
Table: ETCHANTS

MATERIALS	ETCHANTS
SG iron-I and SG iron-II	10 % Nital, swab
316 SS and 304 SS 28% Chromium Iron (As Cast and HT)	10% oxalic acid at 0.5 A current and 5V Voltage, 20 secs.
Tungsten carbide-cobalt coatings (88-12%)	Murakami Reagent (10gms $K_4FeCN_6$ +10gms NaOH+10gms $H_2O$ ), Swabbed for 2 minutes.

**Results and discussions**

**Analysis of high stress abrasion**

Results of the six monolithic materials and WC-Co coatings (prepared using JK112 and WOKA powders, at 45 psi chamber pressure) studied under two body high stress test condition are presented. The applied load was the only variable in all the groups of the test, and the sliding speed and the wear path were kept constant. The standard testing condition was 20N applied load, 50mm/s sliding speed and 6m wear path.



Mag 200X

a)



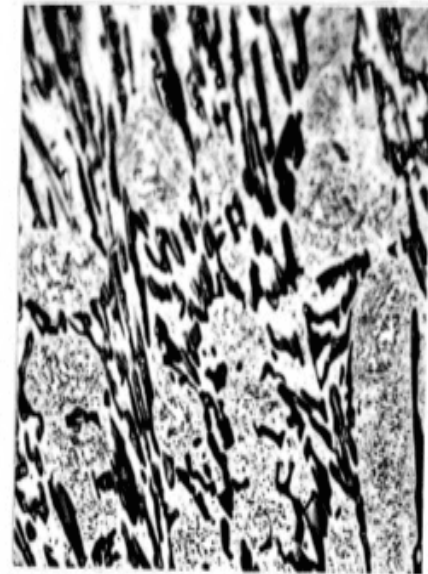
Mag 400X

b)

28% chromium (as cast) iron



Mag 200X



Mag 400X

28% chromium (heat treated) iron

Figure 5.1: Photomicrographs showing the structure of 28% chromium (as cast and heat treated) iron . The heat treated structure clearly indicates the finely dispersed carbides.



Mag 100X

a)



Mag 400X

b)

SG iron-I



Mag 100X

c)

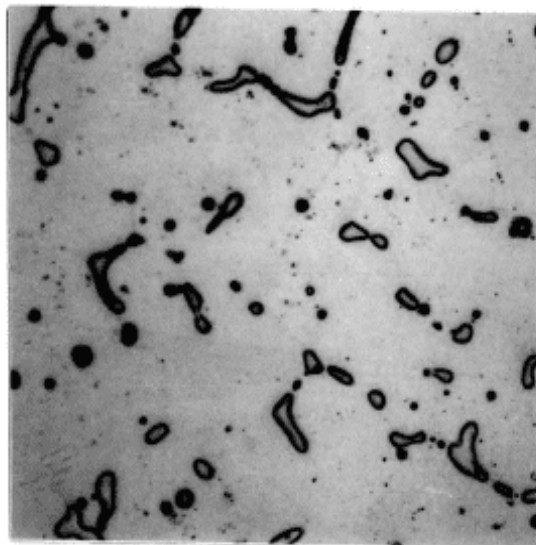


Mag 400X

d)

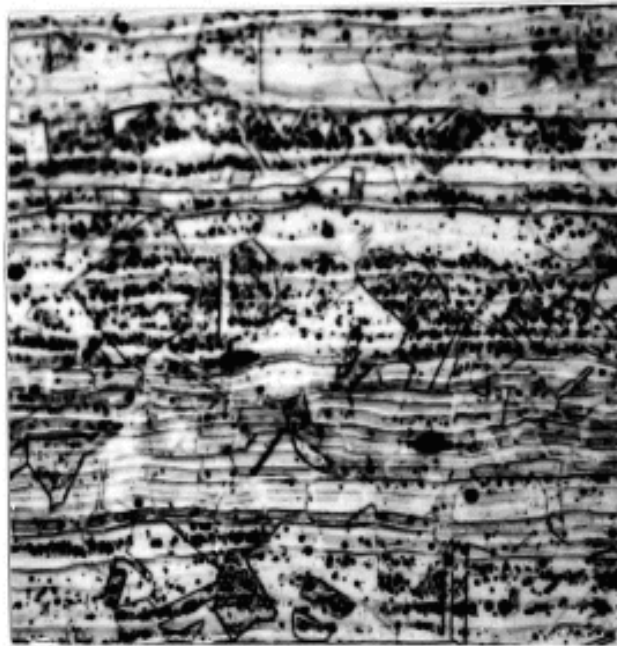
**SG iron-II**

**Figure: Photomicrographs showing the structure of SG iron-I and SG iron-II. The difference between the matrix is clearly observed. The SG iron-I indicates large amounts of ferrite in the matrix**



Mag 200X

a) 304SS

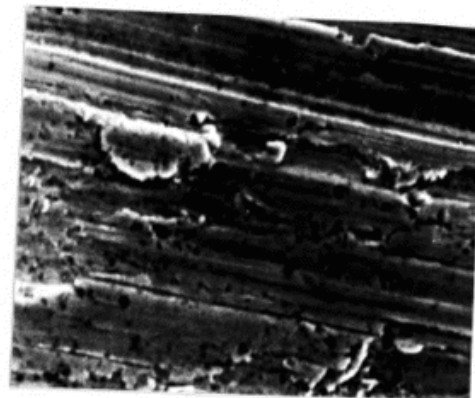


b) 316SS

Figure: Photomicrographs showing the structure of 304SS and 316SS. The ' 304SS indicates a cast dendritic structure, a) cast structure showing carbide precipitation (overetched), b) structure showing 100% FCC austenite grains and the bands represent plastic deformation. Black spots are etching artefacts

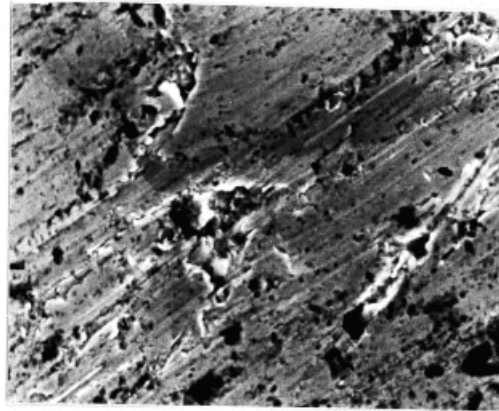


a) 316SS

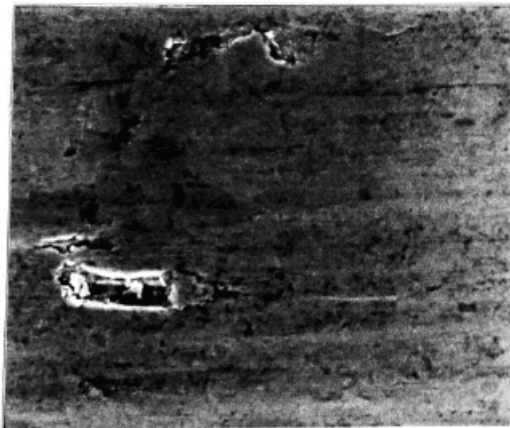


b) 304SS



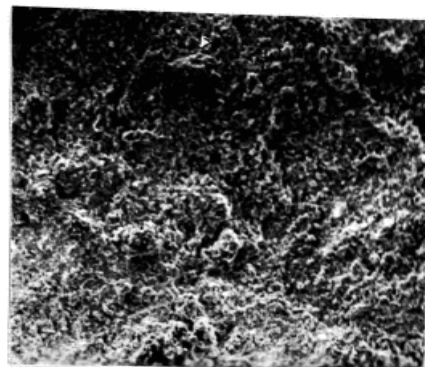


c) SG iron-II



d) 28% Chromium iron (as cast)

Figure : Photomicrographs showing topography of the worn surface after dry " sand rubber wheel abrasion test (Procedure-A).Mag 1.2 KX. a) ductile flow of material representing microploughing, b) microchips observed on the surface representing microcutting, c) detached wear debris showing microcracking, d) displaced prow showing a cutting action.



Mag 800X  
Dense WC-Co coating



Worn Coating



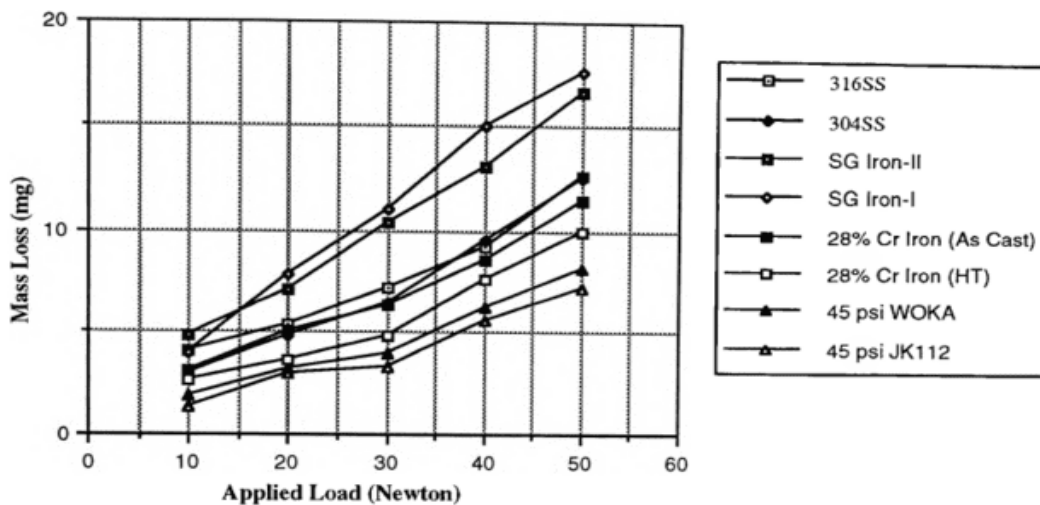
Unworn Coating

Figure: Photomicrograph of wear scar of tungsten carbide cobalt coating (JK112) after RWAT, and the unworn coating

**Effect of Applied Load**

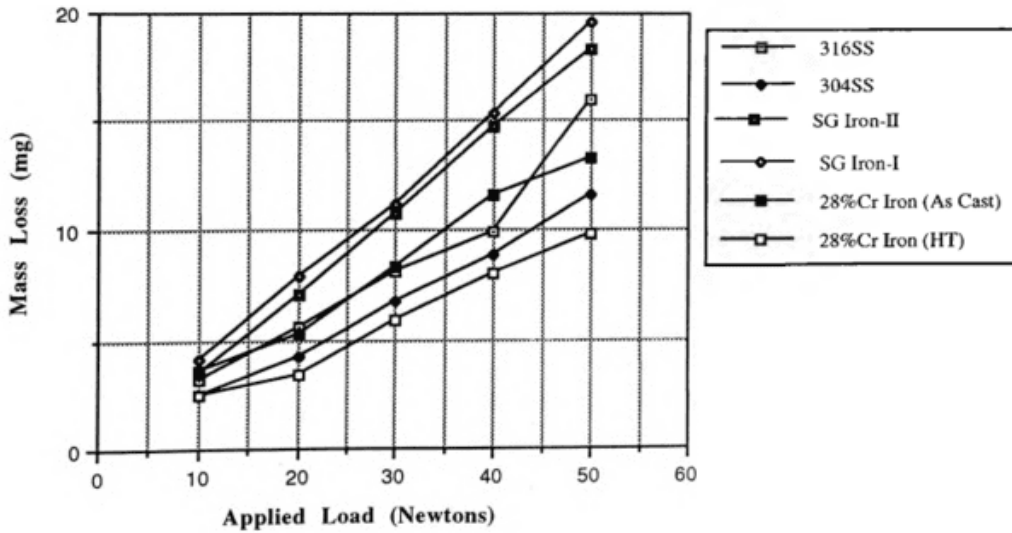
Relationship between mass loss and applied load from ION to 50N, 50mm sliding speed and 6m wear path are shown in Figure, for SiC abrasive, Figure for alumina abrasive, and Figure for garnet abrasive. Figure shows that mass loss increases with load, for all the six monolithic materials. The SG iron-I showed the highest mass loss and 28% chromium (heat treated) iron showed the lowest. Nonlinearity between mass loss and load was observed for all the materials, and at ION load, the mass loss of SG iron-E was found to be greater than SG iron-I. The WC-Co coating prepared from JK112 source showed a lower mass loss than the coating prepared from WOKA source. Figure shows that the mass loss of SG iron-I is the highest and 28% chromium (heat treated) iron is the lowest, for 120# alumina abrasive, similar to the results obtained using SiC abrasive. The mass loss however was higher for the alumina abrasive than for the SiC abrasive. The notable feature was the lower mass loss of 304SS compared to 28% chromium (as cast) iron. Figure shows that the mass loss of SG iron-II is the highest and 28% chromium (heat treated) iron is the lowest, for garnet abrasives. The relationship between the mass loss and applied load was however nonlinear, for each of the three abrasives. For the different abrasives it is clear that the 28% chromium (heat treated) iron has the lowest mass loss, among the monolithic materials that were studied

**High Stress Abrasion Test Results.**  
 Conditions : V=50mm/sec, Path 6m, 180#SiC Abrasive.



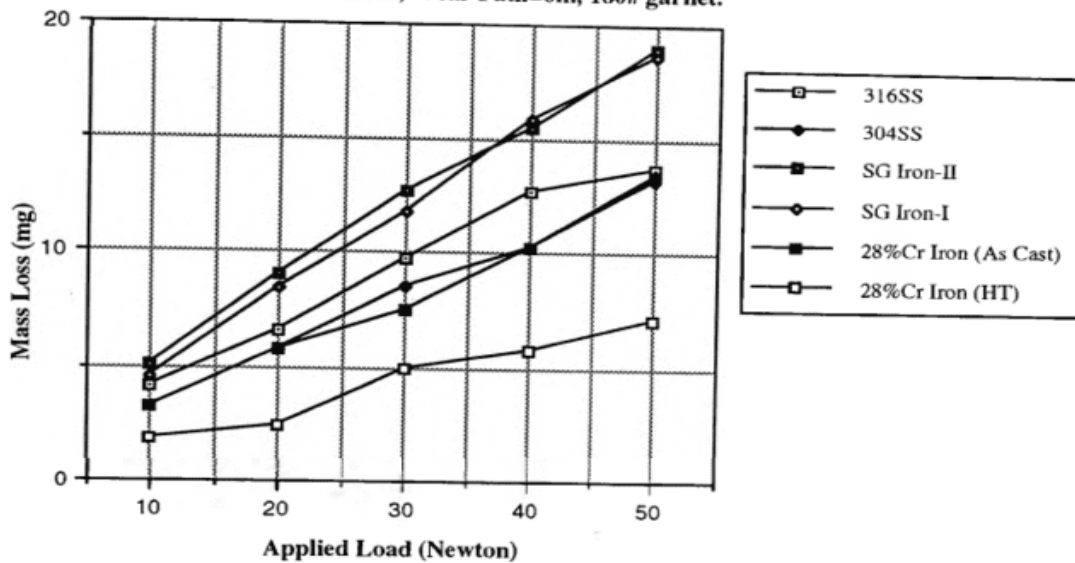
Graph: Diagram showing mass loss and applied load for Silicon Carbide abrasive

**HIGH STRESS ABRASION TEST RESULTS.**  
 CONDITIONS: V=50mm/sec, wear path=6m, 120# Alumina.



Graph: Diagram showing mass loss and applied load for alumina abrasive.

**HIGH STRESS ABRASION TEST RESULTS.**  
 CONDITIONS: V=50mm/sec, Wear Path=6m, 180# garnet.



Graph: Diagram showing mass loss and applied load for garnet abrasive

### III. CONCLUSION

An original design of a pin-on-disk tribometer is presented for the analysis of the behaviour of abrasive grains in the grinding processes conditions. The achieved contact conditions are close to those of the real grinding process. This consideration allows the extrapolation of results obtained on the pin-on-disk tribometer to the design of industrial grinding wheels for a specific grinding operation. Grinding contact conditions are imposed and thoroughly controlled on the tests carried out in the pin-on-disk tribometer with the aim of differentiate wear behaviour of two types of alumina crystalline structure:



## REFERENCES

1. D.Forsström a b(2016)"Calibration and validation of a large scale abrasive wear model by coupling DEM-FEM: Local failure prediction from abrasive wear of tipper bodies during unloading of granular material", Engineering Failure Analysis,ISSNno:1350-6307,Vol.66,Pages:274-283,<https://doi.org/10.1016/j.engfailanal.2016.04.007>
2. Q Chen(2003)"Computer simulation of solid-particle erosion of composite materials",Wear,Vol.255,Issues.1–6,Pages:78-84,[https://doi.org/10.1016/S0043-1648\(03\)00065-6](https://doi.org/10.1016/S0043-1648(03)00065-6)
3. Rajaneesh N. Marigoudar (2011)"Dry Sliding Wear Behaviour of SiC Particles Reinforced Zinc-Aluminium (ZA43) Alloy Metal Matrix Composites", Journal of Minerals and Materials Characterization and Engineering,Vol.10,No.5, pages:419-425, doi: 10.4236/jmmce.2011.105031
4. S. I. Maldonado-Ruiz (2014)"Effect of V-Ti on the Microstructure and Abrasive Wear Behavior of 6CrC Cast Steel," Balls. Journal of Minerals and Materials Characterization and Engineering,ISSNno:2327-4085,Vol.2, No:05, Pages.383-391. Doi:10.4236/jmmce.2014.25043.
5. S. Rau a(2018)"Multi-phase simulation of pneumatic conveying applying a hydrodynamic hybrid model for the granular phase",PowderTechnology,ISSN NO:Vol.330,Pages:339-348,<https://doi.org/10.1016/j.powtec.2018.02.041>
6. Sixing Liu a c d(2023)"Wear characteristics of brazing diamond abrasive wheel on high efficiency grinding ferrous metals", Wear,ISSNno:0043-1548,Vol.514–515, pages:204-580, <https://doi.org/10.1016/j.wear.2022.204580>
7. Sunday A. Afolalu (2019)"Modelling and Simulation of Mechanical Wear of Carburized Cutting Tool",Procedia Manufacturing,Volume.35,Pages:1067-1072,<https://doi.org/10.1016/j.promfg.2019.06.058>.
8. Tomas De la Mora Ramirez (2020) "Numerical Model of Ultra-High Molecular Weight Polyethylene Abrasive Wear Tests". Modeling and Numerical Simulation of Material science,ISSNno:2164-5353,Vol.10,No.1, pages:1-14,Doi:10.4236/mns.ms.2020.101001.
9. Mohd Shadab Khan (2014) "Statistical Analysis for the Abrasive Wear Behavior of Al 6061." Journal of Minerals and Materials Characterization and Engineering, ISSN No: 2327-4085Vol.2, No.4, pages: 292-299. Doi:10.4236/jmmce.2014.24034.
10. Benjamin A. Kotzur(2018)"Particle attrition mechanisms, their characteri sation, and application to horizontal lean phase pneumatic conveying systems: A review",Powder Technology,ISSNno.0032-5910,Vol.334,Pages:76-105, <https://doi.org/10.1016/j.powtec.2018.04.047>



INTERNATIONAL  
STANDARD  
SERIAL  
NUMBER  
INDIA



## International Journal of Advanced Research in Arts, Science, Engineering & Management (IJARASEM)

| Mobile No: +91-9940572462 | Whatsapp: +91-9940572462 | [ijarase@gmail.com](mailto:ijarase@gmail.com) |

[www.ijarase.com](http://www.ijarase.com)